EXPERIMENTAL STUDY OF THERMAL CONDUCTIVITY OF CROSS-LAMINATED TIMBER PANEL NARROW EDGES

Edvins Grants[1], Uldis Gross[2], Viktorija Strausina[2]
[1]Forest and Wood Products Research and Development Institute, Latvia;
[2]Latvia University of Life Sciences and Technologies, Latvia
edvins.grants@e-koks.lv , uldis.gross@lbtu.lv

Abstract. This study investigates the thermal conductivity of cross-laminated timber (CLT) samples made of Norway spruce when heat flow occurs parallel to the main plane of the panel. Due to the layered nature of CLT, heat transfer occurs both along and across the grain, depending on lamella orientation. The objective was to assess whether thermal conductivity varies with different proportions of end-grain in the heat flow path – relevant for construction elements such as building corners or foundation joints. Three CLT sample types were prepared with controlled end-grain proportions: Group 1 with 50.0%, Group 2 with 64.8% and Group 3 with 34.5%. Samples were conditioned at 20 °C and 65% relative humidity (RH). Thermal conductivity (λ) was measured using a HFM 436/3 device under steady-state conditions at 10°C, 20°C and 23 °C, with a 10°C temperature gradient. The results show a clear relationship between end-grain proportion and thermal conductivity. Higher end-grain content (63.8%) yielded higher λ-values, while lower content (34.5%) reduced conductivity, indicating greater thermal resistance. This highlights the anisotropic nature of CLT and the need to consider grain direction in thermal calculations. Exposed panel edges with high end-grain content may cause localized heat loss and increase the risk of condensation, mould, or blue stain. Further modelling is needed to evaluate the impact on overall thermal performance and durability.

Keywords: cross-laminated timber (CLT); thermal conductivity; end-grain proportion; Norway spruce.

Introduction

This study was motivated by the work of Kollmann, as presented in the comprehensive overview by Siau. Their findings established that wood displays significantly different thermal conductivity values along and across the grain, a consequence of its anisotropic cellular structure [1-3]. This phenomenon is not only fundamental in wood science, but it also raises questions about its implications in modern engineered wood products such as cross-laminated timber (CLT) and glued laminated timber (GLT).

Recent experimental studies [4; 5] have confirmed that thermal conductivity of wood varies predictably as a function of grain angle, validating the use of anisotropic models. Despite this, design practices for engineered timber products such as CLT tend to rely on simplified, isotropic assumptions when determining stedy-state thermal performance [6; 7].

Notably, structural design standards such as EN 1995-1-2 account for the directional dependency of thermal degradation during fire exposure, acknowledging that wood burns faster parallel to the grain [8]. Yet, thermal performance in normal service conditions is often treated isotropically in design guidelines, including ISO 10456 and ISO 10077-2 [9; 10], where thermal conductivity values are assigned uniformly. This simplification may be acceptable for conventional light-frame timber construction, where end-grain exposure is minimal. However, in large-scale mass timber elements – such as CLT and GLT panels – the end-grain surfaces can constitute a significant proportion of the exposed area, particularly at wall corners or floor-to-wall junctions.

Recent work, such as Kalbe et al. [11], has begun addressing moisture safety risks associated with exposed end-grain in CLT, highlighting anisotropic absorption effects and their implications for mould growth. Yet, little is known about the thermal performance implications of end-grain exposure in CLT. Studies like Díaz et al. [12] have advanced multiscale modelling approaches for predicting thermal conductivity in wood, but they have not specifically addressed layered configurations where grain directions alternate.

To explore this issue, a controlled experimental campaign was conducted to compare thermal conductivity in CLT samples with varying proportions of end-grain in the heat flow direction. The objective was to determine whether end-grain exposure leads to a measurable increase in thermal conductivity under steady-state conditions. The findings may inform both simulation models and construction detailing practices, especially as the use of exposed mass timber expands in sustainable performance buildings.

This work is intended as a pilot investigation, providing empirical data to assess whether the anisotropic nature of wood – and specifically end-grain orientation – deserves greater consideration in thermal modelling of mass timber elements.

Materials and methods

The test samples in this study were manufactured from industrially produced cross-laminated timber (CLT) panels made of Norway spruce (*Picea abies L.*), which have been previously used in related experimental research. According to manufacturers declaration, the panels are produced of strength graded timber according to EN 14081-1 (characteristic strength class – C24 acc. EN 338) and lamellas are glued together with type I (EN 301) polyurethane (PU) adhesive, intended for structural use. To prepare the samples, the CLT panels were cut into 60 mm wide and 290 mm long strips using a panel saw. The strips were reassembled and bonded into samples, designed to represent three distinct lamination configurations relevant to in-plane thermal conduction.

- Group 1, Fig. 1: All lamellae oriented perpendicularly in alternating layers, creating a symmetric crosswise layout.
- Group 2, Fig. 2: Paired lamellae in the same direction with outer layers aligned parallel to the heat flow direction.
- Group 3, Fig. 3: The same core as Group 2, but with outer layers oriented perpendicularly to the heat flow direction.

The bonded CLT segments were cut to dimensions of approximately 290 mm long and 240 mm wide. Planed using dual-sided thickness planer to ensure smooth and even surfaces for optimal thermal contact with measuring plates in the NETZSCH HFM 436/3 Lambda heat flow meter [13]. The final thickness of each sample was measured, and the exposed end-grain area on the wide surface (in contact with the measurement plates) was calculated as a percentage of the total surface area based on precise dimensional measurements.

Fig. 1. **Group 1 sample ley-up, exposed end-grain 50.0% (*n* = 8)**

Fig. 2. **Group 2 sample lay-up, exposed end-grain 64.8% (*n* = 5)**

Fig. 3. **Group 3 sample lay-up, exposed end-grain 34.5% (*n* = 5)**

All samples were conditioned at 20 °C and 65% relative humidity (RH) until a constant mass was achieved, which corresponds to the reference conditions specified in ISO 10456 for declared values of solid wood materials [9].

The moisture content was determined prior to testing using a resistance-type Brookhuis FMD (v 5.0) moisture meter equipped with insulated pin electrodes, Fig. 4. Wood moisture content (MC) measurements were done inserting electrode pins close to the centre of the sample in approximate 30 mm depth. Measurements were done from both sides as recommended in EAD 130005-00-0304 [14].

Thermal conductivity measurements were performed using NTZSCH HFM 436/3 Lambda heat flow meter device under steady state conditions. The specimens were placed between the hot and cold plates of the meter, and measurements were conducted at equilibrium temperatures of 10 °C, 20 °C, and 23 °C, each with 10 °C temperature differential (ΔT), in accordance with the guidance of ISO 10456, which recommends 10℃ or 23℃ as reference temperatures for testing under steady-state conditions [9]. The inclusion of 20℃ served to compare the declared condition with standard test points and explore whether temperature or moisture content has stronger influence on thermal conductivity in CLT elements.

Fig. 4. **Brookhuis wood moisture content measuring device used for indicative measurements**

Sample density (ρ) was calculated as the ratio between sample mass and volume. Mass was determined using a digital scale (0.1 g resolution), and geometric dimensions were measured using a digital calliper (0.01 mm resolution). Although absolute calibration of the equipment was not performed, the precision was considered sufficient for comparative evaluation. Mean densities ($\bar{\rho}$) and their standard deviations (SD) and standard errors are reported for each group to support regression analysis.

Data from 18 conditioned specimens were analysed. Microsoft Excel was used for data compilation and descriptive data analysis, while in-depth statistical analysis was performed using R 4.4.3 in Rstudio 2024.12.1 + 563. The analysis included regression modelling, as well as ANOVA.

Results and discussion

Table 1 presents a summary of the measured thermal conductivity values (λ) at each equilibrium temperature and density (ρ) for each End-grain group, including mean values, standard deviations (SD) and the standard error (SEM), and the range observed (Min, Max) for the number of samples (n). The results reveal a consistent trend: the samples with higher proportion of end-grain (64.8%) exhibited higher thermal conductivity than those with lower proportions (34.5%), across all tested temperatures.

Table 1

Summary of thermal conductivity (λ) measurements for CLT samples with varying end-grain proportions at different equilibrium temperatures

End-grain group	Equilibrium temperature, °C	Mean thermal conductivity, $\bar{\lambda}$, W·(m·K)$^{-1}$	*SD*, *SEM*	Min	Max	n	Mean density $\bar{\rho}$, kg·m^{-3}	*SD*, *SEM*
1 (50.0%)	10	0.193	0.014, (0.005)	0.174	0.212	8	448.8	14.9, (5.3)
1 (50.0%)	20	0.204	0.017, (0.006)	0.180	0.225			
1 (50.0%)	23	0.202	0.016, (0.006)	0.179	0.218			
2 (64.8%)	10	0.207	0.019, (0.008)	0.185	0.227	5	445.2	10.2, (4.6)
2 (64.8%)	20	0.215	0.019, (0.008)	0.192	0.237			
2 (64.8%)	23	0.218	0.019, (0.008)	0.196	0.240			
3 (34.5%)	10	0.163	0.007, (0.003)	0.157	0.173	5	452.3	25.9, (11.6)
3 (34.5%)	20	0.167	0.007, (0.003)	0.160	0.176			
3 (34.5%)	23	0.168	0.007, (0.003)	0.161	0.179			

This relationship is further illustrated in Fig. 5, where boxplots show the distribution of λ across the three grain configurations at each equilibrium temperature. The boxplots highlight both the variation within each group and the clear difference in median values between end-grain configuration groups.

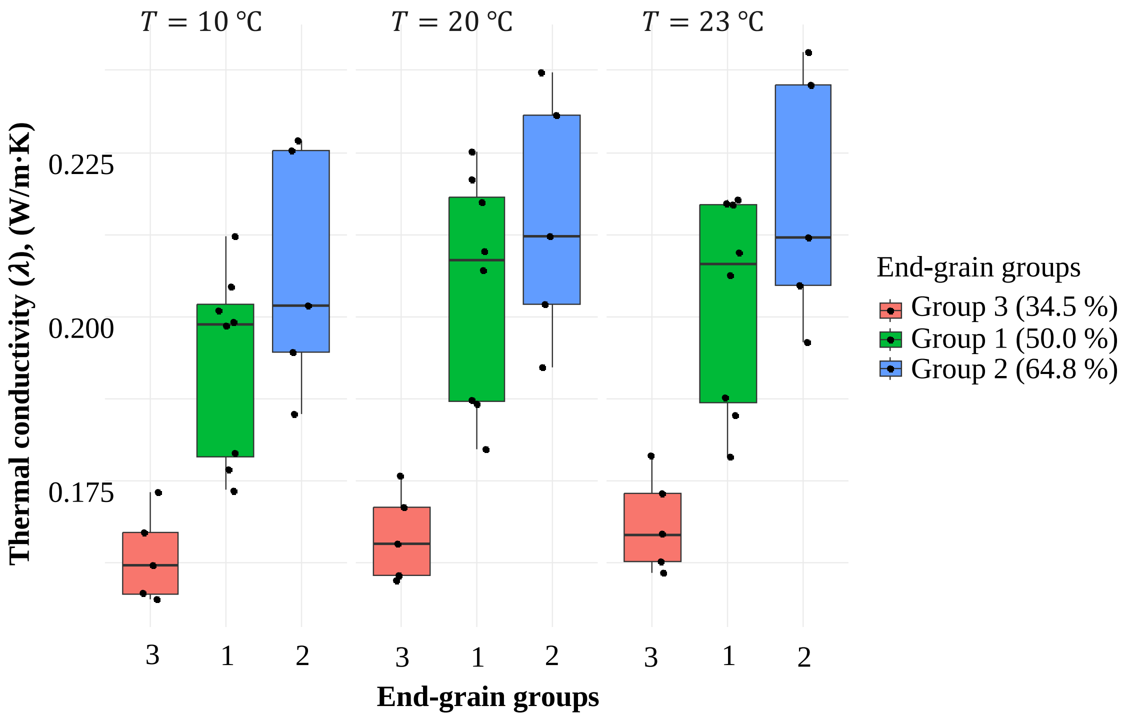

Fig. 5. **Thermal conductivity (λ) by end-grain group and measurement equilibrium temperature (T)**

Statistical analysis using on-way ANOVA confirmed that these differences were significant at each temperature ($p < 0.01$), and subsequent Tukey post-hoc tests further indicated that the greatest differences occurred between the 34.5% (Group 3) and 64.8% (Group 2) end-grain groups. No significant difference was found between 64.8% (Group 2) and 50.0% (Group 1).

Table 2

ANOVA and Tukey HSD results by steady-state equilibrium temperature

Equilibrium temperature, T, °C	Comparison between end-grain groups	Mean difference, W·(m·K)$^{-1}$	95% CI (Lower; Upper)	Adjusted p-value	Significance
23	1 vs. 3	0.034	0.011; 0.057	0.0042	$p < 0.05$
23	2 vs. 3	0.049	0.024; 0.075	0.0004	$p < 0.05$
23	2 vs. 1	0.016	-0.007; 0.038	0.2213	$p > 0.05$
20	1 vs. 3	0.038	0.014; 0.061	0.0021	$p < 0.05$
20	2 vs. 3	0.048	0.022; 0.074	0.0006	$p < 0.05$
20	2 vs. 1	0.011	-0.013; 0.034	0.4845	$p > 0.05$
10	1 vs. 3	0.030	0.009; 0.051	0.0062	$p < 0.05$
10	2 vs. 3	0.043	0.020; 0.067	0.0006	$p < 0.05$
10	2 vs. 1	0.014	-0.007; 0.035	0.2469	$p > 0.05$

The results are graphically illustrated in Fig. 6, the pairwise differences between group means as shown with 95% confidence intervals. The red dashed line at zero represents the threshold of no statistically significant difference; confidence intervals crossing this line indicate that the compared group means do not differ significantly ($p > 0.05$).

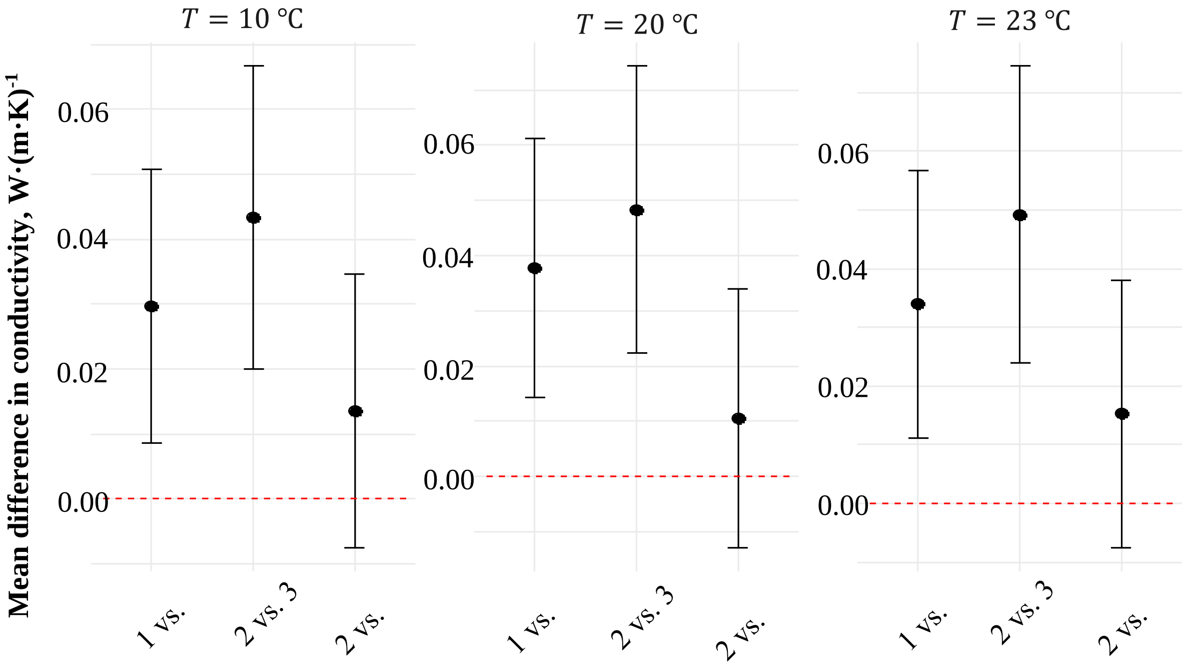

Fig. 6. **Tukey HSD: Pairwise comparisons of thermal conductivity between end-grain groups at each equilibrium temperature**

A separate ANOVA and Tukey HSD analysis was conducted to evaluate the influence of temperature within each group. Although thermal conductivity slightly increased with the temperature, none of the observed differences were statistically significant within groups ($p > 0.3$), indicting that temperature had a minor effect in the tested range. Analysis graphical summary is shown in Fig. 7.

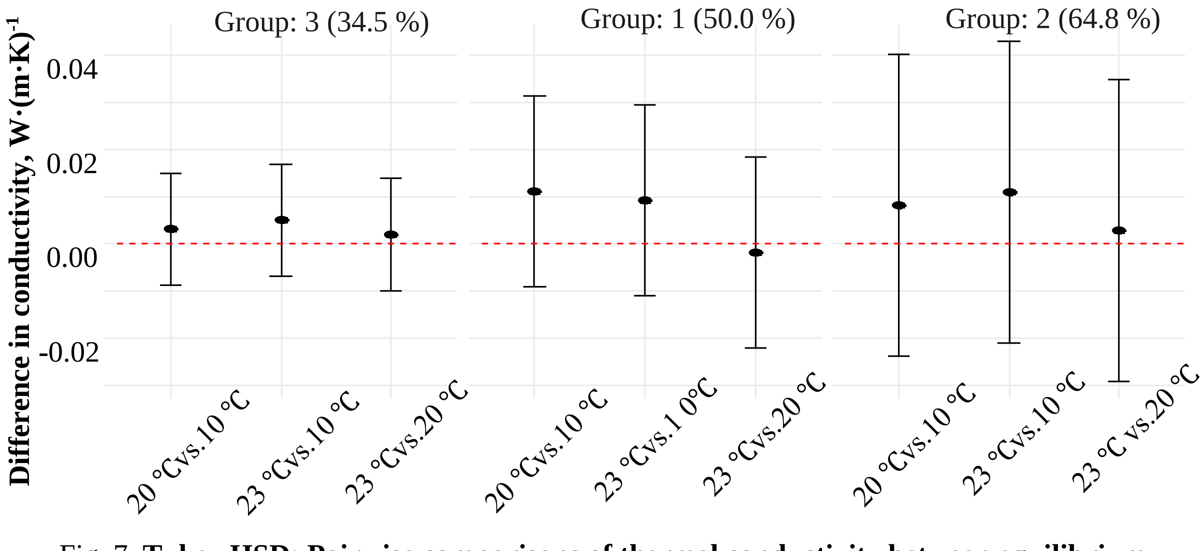

Fig. 7. **Tukey HSD: Pairwise comparisons of thermal conductivity between equilibrium temperatures within each end-grain group**

Regression analysis, Table 3 and Fig. 8, revealed strong correlations between thermal conductivity and density in groups with higher end-grain proportions. Fig. 8 shows the scatterplots with fitted regression lines for λ as a function of density, separated by groups. The regression equations and R^2 values are included for each group.

Overall, the results demonstrate that end-grain orientation plays a more dominant role in influencing thermal conductivity than either density or moisture content, especially when the end-grain surface area exceeds 50%. This supports the hypothesis that traditional thermal modelling approaches, which assume isotropic conduction, may underestimate the heat flow in certain CLT configurations. The findings underscore the need for refined modelling techniques that consider the directional behaviour of heat conduction in massive timber structures.

Table 3

Linear regression of sample density and moisture content for each end-grain group

Group	Term	Estimate	Std. Error	*t*-value	*p*-value	R^2
3	Intercept	0.1098	0.0324	3.39	4.85E-03	0.189
3	Density, kg·m^{-3}	0.0001	0.0001	1.74	1.05E-01	0.189
2	Intercept	-0.4186	0.1599	-2.62	2.13E-02	0.547
2	Density, kg·m^{-3}	0.0014	0.0004	3.95	1.66E-02	0.547
1	Intercept	-0.1377	0.0697	-1.71	1.02E-01	0.444
1	Density, kg·m^{-3}	0.0008	0.0002	4.12	3.80E-04	0.444
3	Intercept	0.323	0.029	11.26	4.46E-08	0.697
3	MC, %	-0.014	0.003	-5.47	1.07E-03	0.697
2	Intercept	0.079	0.186	0.43	6.71E-01	0.038
2	MC, %	0.012	0.016	0.72	4.85E-01	0.038
1	Intercept	0.356	0.072	4.97	5.90E-04	0.181
1	MC, %	-0.013	0.005	-2.21	3.98E-02	0.181

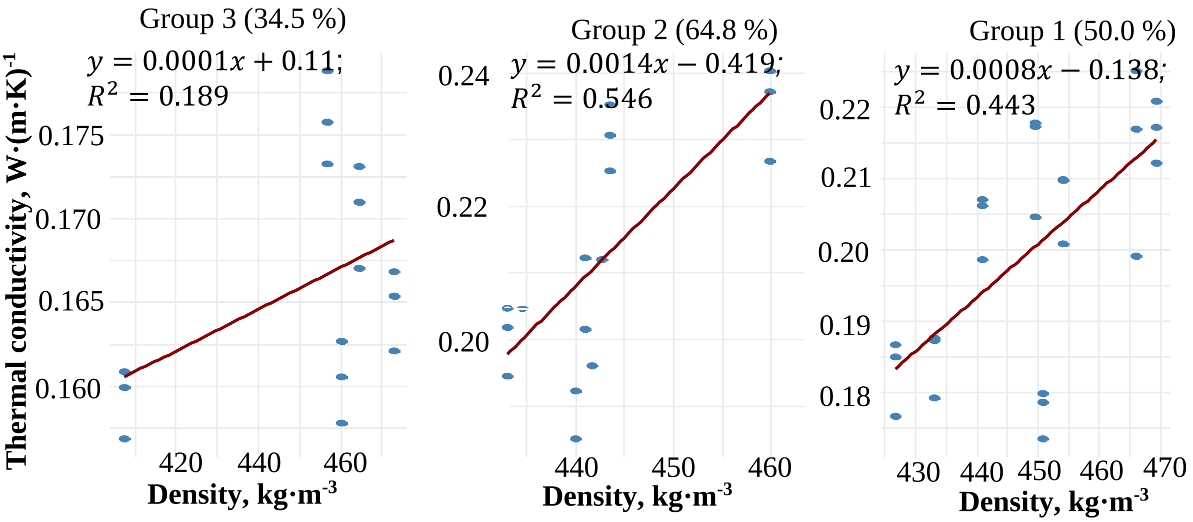

Fig. 8. **Thermal conductivity linear dependency of sample density at each of end-grain groups**

Conclusions

1. Thermal conductivity of CLT increases with a higher proportion of end-grain exposure in the direction of heat flow.
2. Statistically significant differences were observed between groups with 34.5% (Group 3) and 64.8% (Group 2) end-grain area, confirming the influence of grain orientation on in-plane thermal performance.
3. Temperature variation in the tested range (10 to 23 °C) had minimal effect on thermal conductivity.
4. Correlations between thermal conductivity and density were strong in groups with high end-grain proportions, while moisture content showed variable effects depending on group configuration.
5. The results highlight the need for further investigation to refine current modelling approaches and detailing practices to account for anisotropic heat transfer in CLT elements, particularly where end-grain is exposed in larger areas.
6. Further studies should include broader sample sets and explore a wider range of configurations to improve predictive accuracy in design tools for mass timber buildings.

Acknowledgements

In accordance with the contract No. 5.1.1.2.i.0/1/22/A/CFLA/007 between the “Forest Sector Competence Centre of Latvia” Ltd. and the Central Finance and Contracting Agency, the study is conducted by "Meža un koksnes produktu pētniecības un attīstības institūts" Ltd. With support from the European Regional Development Fund (ERDF) within the framework of the "Forest Sector Competency Centre" project P13 – "Investigation of Timber Construction Utilization Possibilities for Specific Agricultural Production Buildings".

Author contributions

Conceptualization, methodology, data analysis and writing: EG; Supervision and experimental assistance: U.G. and V. S. All authors have read and agreed to the published version of the manuscript.

References

[1] MacLean J. D. "Thermal Conductivity of Wood," Heat Piping Air Cond, vol. 13, no. 6, 1941, pp. 380-391.
[2] Siau J. F. "A Geometrical Model for Thermal Conductivity," Wood Science, vol. 3, no. 1, 1970, pp. 38-43.
[3] Kollmann F., Côté W. A. Principles of wood science and technology. I. Solid wood. Berlin, Heidelberg: Springer-Verlag, 1968.
[4] Vay O., De Borst K., Hansmann C., Teischinger A., Müller U. "Thermal conductivity of wood at angles to the principal anatomical directions," Wood Sci Technol, vol. 49, no. 3, May 2015, pp. 577-589. DOI: 10.1007/s00226-015-0716-x.
[5] Avramidis S., Lazarescu C., Rahimi S. "Basics of Wood Drying," in Springer Handbooks, Springer Science and Business Media Deutschland GmbH, 2023, pp. 679-706. DOI: 10.1007/978-3-030-81315-4_13.
[6] Artun H., Lakot Alemdağ E., "The Effect of Cross-Laminated Timber (CLT) Material on Building Heating-Cooling Loads in a Temperate Humid Climate Zone," Gazi University, Journal of Science, Part B: ART, HUMANITIES, DESIGN AND PLANNING, vol. 11, no. 1, 2023, pp. 47-60. [online] [11.02.2025]. Available at: http://dergipark.gov.tr/gujsb
[7] Salonvaara M., Desjarlais A. "Impact of Insulation Strategies of Cross-Laminated Timber Assemblies on Energy Use, Peak Demand, and Carbon Emissions," Buildings, vol. 14, no. 4, Apr. 2024, DOI: 10.3390/buildings14041089.
[8] CEN, "EN 1995-1-2: Eurocode 5: Design of timber structures - Part 1-2: General - Structural fire design," Brussels, 2008.
[9] International Organization for Standardization, "Building materials and products - Hygrothermal properties - Tabulated design values and procedures for determining declared and design thermal values (ISO 10456)," Geneva, Switzerland., 2007. Accessed: Mar. 17, 2025. [Online]. Available: https://www.iso.org/standard/40966.html
[10] International Organization for Standardization, "Thermal performance of windows, doors and shutters – Calculation of thermal transmittance Part 2: Numerical method for frames (ISO 10077-2)," Geneva, Switzerland, 2017. Accessed: Mar. 17, 2025. [online] [11.02.2025]. Available at: https://www.iso.org/standard/64995.html
[11] Kalbe K., Pärn R., Ruus A., Kalamees T.,"Enhancing CLT construction – Hygrothermal modelling, novel performance criterion, and strategies for end-grain moisture safety," Journal of Building Engineering, vol. 98, Dec. 2024, DOI: 10.1016/j.jobe.2024.111411.
[12] Díaz A. R., Saavedra Flores E. I., Yanez S. J., Vasco D. A., Pina J. C., Guzmán C. F. "Multiscale modeling of the thermal conductivity of wood and its application to cross-laminated timber," International Journal of Thermal Sciences, vol. 144, pp. 79-92, Oct. 2019, DOI: 10.1016/j.ijthermalsci.2019.05.016.
[13] NETZSCH-Gerätebau GmbH., "HFM 436 Lambda: High Precision Instrument for Testing Insulating Materials." Accessed: Mar. 17, 2025. [online] [11.02.2025]. Available at: https://www.netzsch.com
[14] European Organisation for Technical Assessment, "EAD 130005-00-0304, Solid wood slab element to be used as a structural element in buildings," Brussels, Belgium, 2015. Accessed: Mar. 17, 2025. [online] [11.02.2025]. Available at: https://www.eota.eu/download?file=/2013/13-13-0005/ead%20for%20ojeu/ead-130005-00-0304-solid-wood-slab-element-structural-element-in-buildings_ojeu.pdf